EFFECT OF Ti$_2$AlC PARTICLES ON THE MICROSTRUCTURE AND ELEVATED-TEMPERATURE-DEFORMATION PROPERTIES OF γ-TiAl ALLOYS

VPLIV DELCEV Ti$_2$AlC NA MIKROSTRUKTURO IN DEFORMACIJSKE LASTNOSTI ZLITIN γ-TiAl PRI POVIŠANI TEMPERATURI

Tomáš Čegan, Michal Cagala, Miroslav Kursa, Petr Kawulok, Stanislav Rusz, Jan Juřica, Jiřina Vontorová

VŠB-Technical University of Ostrava, Faculty of Metallurgy and Materials Engineering, Department of RMSTC, 17. listopadu 15, 708 33 Ostrava – Poruba, Czech Republic
tomas.cegan@vsb. cz

The γ-TiAl intermetallics with and without amount fractions $x = 0.3$ % of yttrium and with different carbon amount fractions ranging from 0.9 % to 1.6 % were prepared by vacuum-induction melting in a graphite crucible. Different amounts of carbon were obtained by varying the time of melting. The resulting samples had large rod-like carbides with volume fractions 0.6 % to 3.7 % Ti$_2$AlC in the lamellar matrix consisting of the alternating lamellas of γ-TiAl and α_2-Ti$_3$Al phases. It was found that the grain size of the matrix decreases with the increasing volume fraction of Ti$_2$AlC carbides from 430 μm to 35 μm. In addition, finer carbides with a similar composition were observed. Their size was below 1 μm and they appear mainly at the grain boundaries and also inside the lamellar grains. Compression testing revealed that all the samples had a relatively high yield strength at elevated temperature, from 917 MPa to 623 MPa at 600 °C and from 608 MPa to 547 MPa at 800 °C, but the best strength and the best yield strength were found for the sample with the lowest amount of the large rod-like Ti$_2$AlC carbides. From these results it is concluded that the strengthening at an elevated temperature is a result of C in the solid solution and small carbide precipitates rather than of the rod-like Ti$_2$AlC carbides.

Keywords: titanium aluminides, mechanical properties, microstructure, carbides, carbon

Intermetalne zlitine γ-TiAl z množinskim deležem itrija $x = 0,3$ % in brez njega ter z različno vsebnostjo množinskega deleža ogljika od 0,9 % do 1,6 % so bile izdelane z vakuumskim indukcijskim pretaljevanjem v grafitnem lončku. Različne vsebnosti ogljika so bile dobljene pri različnih časih taljenja. Dobljeni vzorci so imeli volumenski delež Ti$_2$AlC od 0,6 % do 3,7 % velikih paličastih karbidov v lamelarni osnovi iz lamel faz γ-TiAl in α_2-Ti$_3$Al. Ugotovljeno je bilo, da se z večanjem volumenskega deleža Ti$_2$AlC-karbidov velikost zrn osnove zmanjšuje od 430 μm do 35 μm. Opazilo se je tudi, da imajo drobnejši karbidi podobno sestavo. Njihova velikost je manjša od 1 μm, pojavljajo se večinoma po mejah zrn in tudi v lamelarnih zrnih. Tlačni preizkus je odkril, da imajo vsi vzorci relativno visoko mejo tečenja pri povišanih temperaturah: od 917 MPa do 623 MPa pri 600 °C in od 608 MPa do 547 MPa pri 800 °C. Najvišjo trdnost in najvišjo mejo tečenja je imel vzorec z najmanjšo vsebnostjo velikih, paličastih Ti$_2$AlC-karbidov. Iz rezultatov je razvidno, da je utrjevanje pri povišanih temperaturah bolj posledica ogljika v trdni raztopini in drobnih karbidnih izločkov kot pa velikih paličastih Ti$_2$AlC-karbidov.

Ključne besede: titanovi aluminidi, mehanske lastnosti, mikrostruktura, karbidi, ogljik

1 INTRODUCTION

The advantages of gamma TiAl-based alloys such as specific modulus, specific high-temperature strength and oxidation resistance makes them attractive candidates for the use as high-temperature structural materials in the automotive, aerospace and power industries[1]. However, a problematic preparation of the final products and their high price present the biggest problem for their higher utilisation. Precise casting is the most cost-effective method for the production of the components from TiAl-based alloys[1]. Unfortunately, gamma TiAl-based alloys cannot be melted in conventional refractory crucibles and skull-melting processes are required to prevent contamination.

It was demonstrated that a small amount of carbon ($x < 0.5$ %) increases the strength of TiAl-based materials at room and elevated temperatures due to the solid-solution hardening or precipitation of fine carbide particles.[2,3] Moreover, TiAl composites with higher shares of carbides also exhibit excellent strength and oxidation resistance at elevated temperatures[4]. Powder metallurgy has been the most frequently used method for the production of TiAl alloys with carbon contents. Additions of TiC powder, graphite or Al/TiC master alloy were tested.[2–5] However, melting in a graphite crucible could be a much cheaper alternative for the preparation of this material. In this work TiAl alloys with different amounts of Ti$_2$AlC carbides were produced using a graphite crucible and their mechanical properties were evaluated.

2 EXPERIMENTAL WORK

The melting of the alloys was performed in a LEYBOLD – HERAEUS IS1/FFF vacuum induction furnace using an extruded graphite melting crucible with the

average density of 1.75 g/cm³, the porosity of 17–20 % and the maximum granularity of 0.8 mm. The charge was composed of formed bits of Ti of 3N purity, bits of Al of 4N purity and in the case of alloys alloyed with yttrium also of bits of yttrium of 3N purity. The alloying with yttrium was used in order to assess the influence of this element on the microstructure. Afterwards four alloys were melted with the nominal compositions of Ti-47Al and Ti-47Al-0.3Y (amount fractions, x/%), which were then cast into a graphite mould. All these processes ran under an atmosphere of argon of 4N5 purity. Different amounts of carbon and carbides were achieved with different times of stabilising the melt ranging from 30 s to 90 s. The final products were the castings with a diameter of 10 mm and a length of 100 mm. The samples for a metallographic investigation using light microscopy (LM), X-ray diffraction analysis (XRD) and scanning electron microscopy in the mode of back-scattered electrons (BSE) and secondary electrons (SE) were taken from the castings. The chemical composition was determined with an energy dispersive analysis (EDS). The amounts of oxygen and carbon were measured with the thermo-evolution method using the ELTRA ONH-2000 and ELTRA CS-2000 analysers. The volume fraction of carbides and grain size were determined with a computerised image analysis.

Mechanical-compression tests were performed on the cylindrical samples with a diameter of 8 mm and a length of 12 mm, which were prepared by electro-spark machining and then turned to the required size on a HAAS- ST10 CNC turning lathe. An HDS-20 simulator of hot deformation was used for mechanical testing at the strain rate of 0.05 s⁻¹. The heating to the required temperature (800, 600, 400) °C was performed at a rate of 3 °C/s and the sample was deformed after a dwell time of 15 s at the required temperature.

3 RESULTS AND DISCUSSION

3.1 Chemical compositions and the amounts of interstitial elements

Table 1 presents the analyzed chemical compositions of the prepared alloys. The compositions of the alloys do not show any significant deviations from the nominal composition. The prepared alloys show a comparatively low amount of oxygen and, in this respect, they satisfy the requirements for the applications of these alloys in the industry, where the maximum admissible mass fraction of oxygen is approximately 0.05 %[6]. An analysis of the carbon amounts in the prepared castings showed that during the melting of TiAl intermetallics in graphite crucibles the amount of carbon increased as a result of its absorption from the walls of a graphite crucible into the melt. The determined values of the carbon amounts in individual samples were, nevertheless, quite different. The highest carbon mass fraction of 0.5 % was found in alloy 1, for which the longest time of stabilisation of the melt was used, namely 90 seconds. The lowest mass fraction was found in alloy 4, namely 0.295 %, for which the time of stabilisation of the melt was 30 s.

3.2 Microstructures and the solidification behaviour

The microstructures of all the prepared alloys were dendritic (**Figure 1**). Dendrites were formed of alternating lamellas of the α_2- and γ-phases. In the interdendritic spaces the γ-phase was observed. **Figure 2** shows a detail of one of the lamellar dendrites (L) with the chemical composition of (53.29 ± 0.81) % Ti and (46.71 ± 0.81) % Al, and also an interdendritic γ-phase, with the average chemical composition of (49.06 ± 1.07) % Ti and (50.94 ± 1.07) % Al (all the results of EDS are given in amount fractions, x/%).
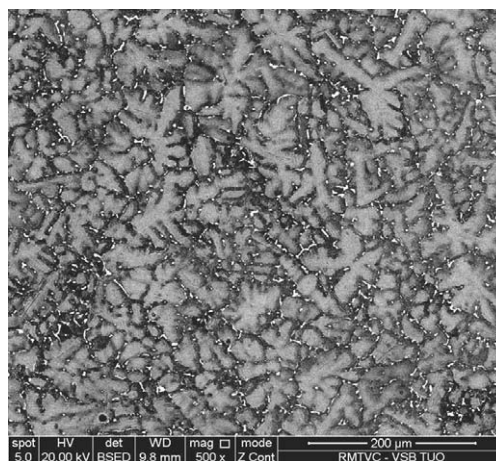

Figure 1: Microstructure of sample 3 (BSE)
Slika 1: Mikrostruktura vzorca 1 (BSE)

Table 1: Chemical compositions, amounts of oxygen, carbon, Ti₂AlC carbides and Y-rich phases (mass fraction, w/%; volume fraction, φ/%; amount fraction, x/%)
Tabela 1: Kemijska sestava, vsebnosti kisika in ogljika ter vsebnost Ti₂AlC-karbidov in faz, bogatih z Y (masni delež, w/%; volumenski delež φ/%, množinski delež, x/%)

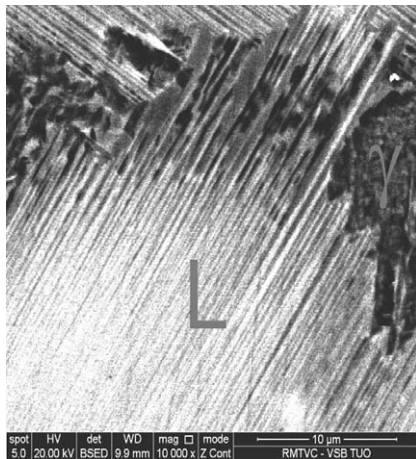| Sample	Measured composition (x/%)			Oxygen (w/%)	Carbon (w/%)	Amount of carbides (φ/%)	Amount of Y-rich phases (φ/%)
	Ti	Al	Y				
1	52.64 ± 0.06	47.36 ± 0.06	0	0.045 ± 0.002	0.500 ± 0.006	3.73 ± 0.82	–
2	52.42 ± 0.18	47.58 ± 0.18	0	0.038 ± 0.003	0.315 ± 0.004	1.28 ± 0.78	–
3	52.15 ± 0.01	47.60 ± 0.09	0.25 ± 0.08	0.033 ± 0.010	0.386 ± 0.009	2.59 ± 0.67	1.60 ± 0.44
4	53.23 ± 0.42	46.39 ± 0.45	0.38 ± 0.06	0.034 ± 0.003	0.295 ± 0.003	0.64 ± 0.28	1.58 ± 0.40

Figure 2: Lamellar-dendrite detail of sample 2 (BSE)
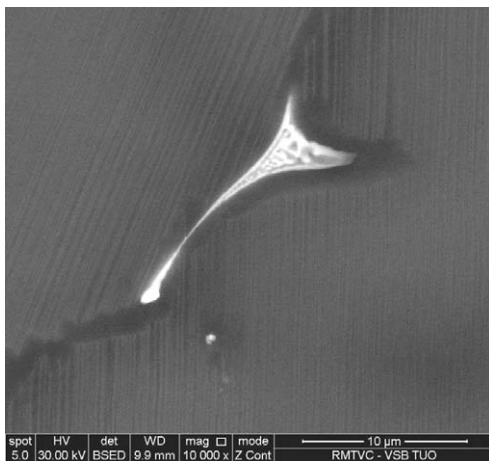**Slika 2:** Lamelarni dendriti vzorca 2 (BSE)

Figure 3: Yttrium-rich phase in sample 4 (BSE)
Slika 3: Faza, bogata z Y, v vzorcu 4 (BSE)

In the alloys alloyed with yttrium we also observed a certain share of the phases rich in yttrium, shown in **Figures 1, 3** and **4** as white areas. They were present in two diffe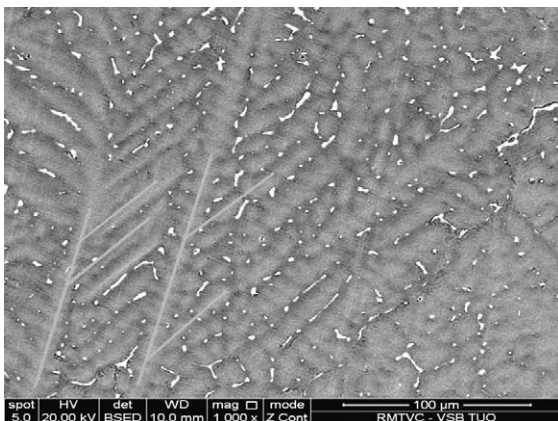rent forms, particularly in the interdendritic spaces and at the grain boundaries. They were also observed, though to a lesser extent, inside the dendrites.

The determined chemical composition of smaller phases of a lighter colour analysed with the EDS method was the following: (19.60 ± 3.84) % Y, (31.18 ± 2.88) % O, (22.95 ± 5.65) % Ti and (26.27 ± 1.90) % Al (x/%). The composition of this phase, therefore, corresponds to Y_2O_3, which was also found with diffraction (not presented), although almost in every particle we also identified the amounts of Ti and Al. This may have been caused by the small size of these particles and the results of the measurements might have been influenced by the environment. The established chemical composition of the larger darker phases rich in yttrium, analysed with the EDS method was the following: (26.44 ± 9.05) % Ti, (55.64 ± 2.15) % Al and (17.92 ± 7.23) % Y (x/%). This phase was identified as YAl_2.

The α-phase was determined as the primary crystallisation phase since dendrite arms have a hexagonal symmetry (with an angle between the dendrite arms of approximately 45°), which corresponds with the solidification of the melt through the α-phase[6]. **Figure 4** shows an example of the α symmetry of dendrites.

3.3 Carbide precipitation

Coarser particles of the acicular type were observed in all the prepared alloys. They typically achieved a diameter of up to 2 μm and their length varied from 10 μm to 150 μm. They were distributed almost uniformly all over the whole areas of the samples' cross-sections; only in the boundary areas their occurrence was slightly lower. **Figure 5** shows an example of these particles. By analysing the chemical compositions (EDS) it was determined that these particles contained $x = (44.41 \pm 2.34)$ % Ti, $x = (24.74 \pm 2.47)$ % Al and $x = (30.85 \pm 3.85)$ % C. The titanium and aluminium amounts were approximately 2 : 1 and a bright display of these particles in the BSE mode indicates the amounts of interstitial elements. For these reasons these particles were identified, probably as Ti_2AlC. The X-ray diffraction patterns
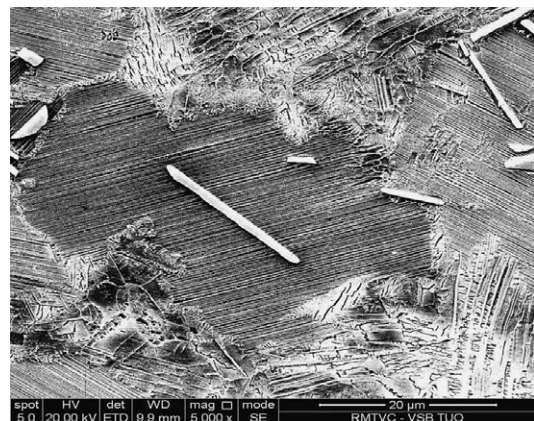

Figure 4: Hexagonal symmetry of dendrites in sample 4 (BSE)
Slika 4: Heksagonalna simetrija dendritov v vzorcu 4 (BSE)

Figure 5: Coarse Ti₂AlC precipitates in sample 1 (SE)
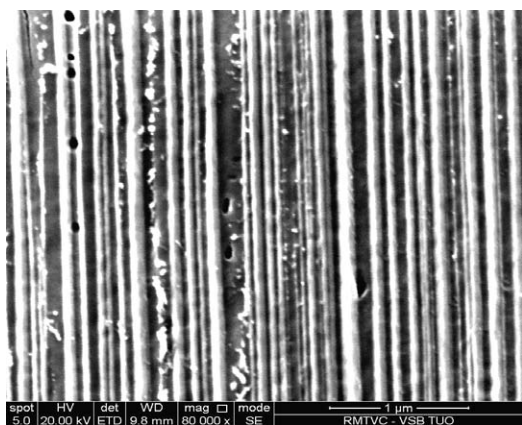**Slika 5:** Grobi izločki Ti₂AlC v vzorcu 1 (SE)

Figure 6: Fine Ti$_2$AlC precipitates in sample 2 (BSE)
Slika 6: Fini izločki Ti$_2$AlC v vzorcu 2 (BSE)

of the selected samples (not presented) also confirmed that the alloys contained, apart from the γ-TiAl and α_2-Ti$_3$Al phases, also the Ti$_2$AlC phase. However, the quantity and size of acicular carbides differed rather significantly between individual samples. The highest

Figure 7: Macrostructure of sample 4
Slika 7: Makrostruktura vzorca 4

Figure 8: Macrostructure of sample 1
Slika 8: Makrostruktura vzorca 1

volume fraction and the largest carbides were found in alloys 1 and 3, in which the highest amount of carbon was also established. In samples 2 and 4 the carbides were observed only in some parts and they were smaller. The amounts of carbides determined with an image analysis are presented in **Table 1**. Carbides were observed particularly inside the primary phase, indicating, according to McCullough[7], together with their bigger size, that they were formed directly from the melt.

In addition to these coarser carbides we also observed finer carbides. Their sizes were up to 1 μm and they were present particularly on the grain boundaries and also inside the lamellar grains. **Figure 6** shows an example of fine carbides. The carbides inside lamellar dendrites were observed primarily in γ-lamellas. However, their small size indicates that unlike the long acicular carbides they were formed from the solid phase and their formation was caused by a small solubility of C in the γ-phase, which was only $x = 0.02$–0.03 %[2].

3.4 Grain size

Figures 7 and **8** show the macrostructures of samples 1 and 4. It is evident already at first glance that alloy 1, which contained $\varphi = 3.73$ % of Ti$_2$AlC carbides, has a much smaller grain size than sample 4, in which the amount fractions of Ti$_2$AlC carbides was only $\varphi = 0.64$ %. The results of determined grain sizes are presented in **Table 2**. It follows from the results that the grain size decreases with the increasing amount of Ti$_2$AlC carbides. The grain-size refinement is caused by the fact that Ti$_2$AlC carbides are the first to crystallise from the melt and that they form nucleation centres for the formation and growth of α-grains, which then transform into a lamellar structure. Smaller deviations of the grain-size values for the samples with higher amounts of carbides also indicate a more regular shape and smaller differences in the grain size. No significant influence of yttrium on the grain size was observed in the alloys alloyed with yttrium.
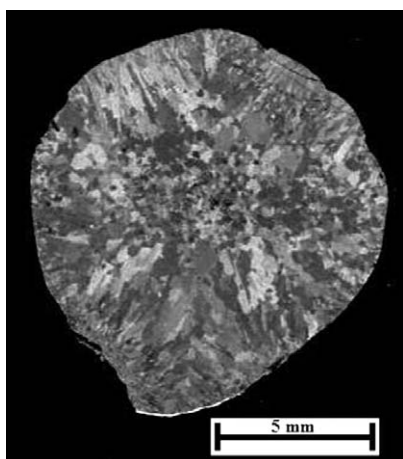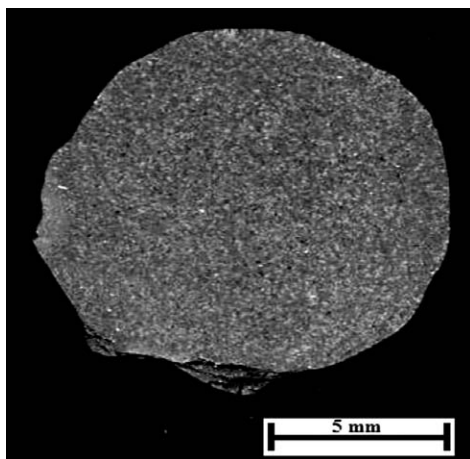
Table 2: Dependence of the amount of Ti$_2$AlC particles on the grain size
Tabela 2: Odvisnost vsebnosti izločkov Ti$_2$AlC od velikosti zrna

Sample	Amount of carbides (φ/%)	Grain size (μm)
1	3.73 ± 0.82	34.40 ± 8.10
2	1.28 ± 0.78	255.99 ± 59.66
3	2.59 ± 0.67	139.26 ± 46.28
4	0.64 ± 0.28	430.58 ± 99.63

3.5 Mechanical properties

Figure 9 presents the curves illustrating the relation between the strain and stress determined at the temperature of 800 °C during the compression mechanical tests for all four alloys. As it can be seen in this figure, all the samples have a similar behaviour at this temperature. The established values of the proof stress did not show
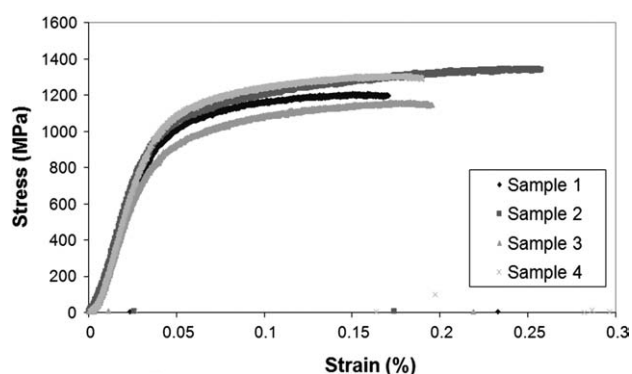
Figure 9: Strain-stress curves at 800 °C
Slika 9: Krivulja raztezek – napetost pri 800 °C

Table 3: Compressive 0.2 yield strength as a function of the test temperature (MPa)
Tabela 3: Tlačna meja tečenja 0,2 v odvisnosti od temperature (MPa)

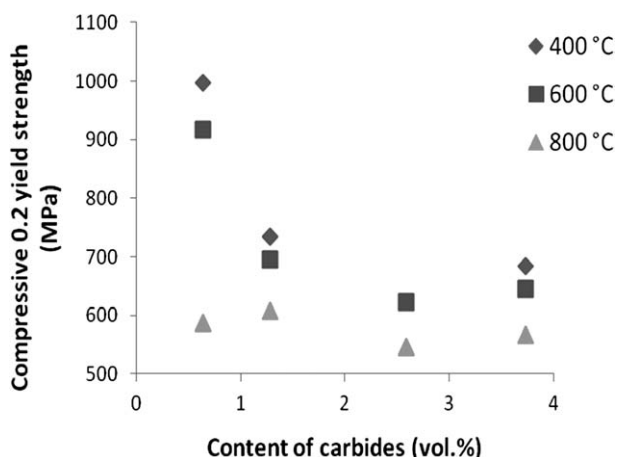| Temperature (°C)	Sample 1	Sample 2	Sample 3	Sample 4
800	566	608	547	588
600	645	695	623	917
400	684	734	-	998

Figure 10: Dependence of the amount of carbides on the compressive 0.2 yield strength
Slika 10: Odvisnost vsebnosti ogljika od tlačne meje tečenja 0,2

any significant differences, ranging from 547 MPa for alloy 3 up to 608 MPa for alloy 2. Bigger differences were, however, found between the determined values of the strength limit. The lowest strength was found for alloy 3, namely, 1158 MPa, and the highest strength was determined for alloy 2, namely, 1350 MPa. This alloy also had the highest achieved ductility, up to 23.5 %. Alloy 1 had the lowest ductility, up to 14.98 %. **Table 3** presents the values of the proof limit analyzed at all the tested temperatures. It follows from the results that the lowest yield strength was achieved for alloys 1 and 3, which had higher amounts of carbon and carbides despite their much smaller grain sizes. The highest values of the yield strength were determined for alloy 4, which had the lowest amounts of carbon and carbides.

The diagram presented in **Figure 10** illustrates the relation between the proof limit at the temperatures of (400, 600 and 800) °C and the determined amounts of carbides in the alloys. It seems from this diagram that if the amount of carbides is higher than $\varphi = 1$ %, the values of the proof limit at (400 and 600) °C are significantly decreased. At the temperature of 800 °C the values of the proof limit are not decreased. From this information it can be, therefore, concluded that larger Ti₂AlC carbides do not have a favourable influence on the mechanical properties of γ-TiAl alloys at these temperatures. Comparatively high values of the yield strength for alloy 4 were probably caused by the strengthening of the solid solution due to carbon and the precipitation of fine carbides.

4 CONCLUSIONS

The alloys were prepared by vacuum-induction melting in a graphite crucible. The melting in this crucible resulted in a contamination with carbon mass fractions ranging from 0.295 % to 0.5 %. Coarser acicular Ti₂AlC precipitates were observed in the alloys as well as finer carbide precipitates. The quantity and size of the acicular precipitates increased with the determined carbon amount. The highest values of the yield strength at the temperatures of (400, 600 and 800) °C were found for the alloys with smaller amounts of acicular carbides.

From these results it is concluded that the elevated-temperature strengthening is a result of C in the solid solution and small carbide precipitates rather than of the rod-shaped coarse Ti₂AlC precipitates.

5 REFERENCES

[1] X. Wu, Intermetallics, 14 (**2006**), 1114–1122
[2] F. Perdrix, Intermetallics, 9 (**2001**), 807–815
[3] W. H. Tian, Intermetallics, 5 (**1997**), 237–244
[4] J. D. Whittenberger, Intermetallics, 2 (**1994**), 167–178
[5] V. Kevorkijan, S. D. Škapin, Mater. Tehnol., 43 (**2009**) 5, 239–244
[6] J. Zollinger, Intermetallics, 15 (**2007**), 1343–1350
[7] C. McCullough, Materials Science and Engineering, 124A (**1990**), 83–101